

Accepted Manuscript

Title: Photocatalytic degradation and mineralization of Tramadol pharmaceutical in aqueous TiO₂ suspensions: Evaluation of kinetics, mechanisms and ecotoxicity

Author: nullaria nullntonopoulou Ioannis Konstantinou



PII: S0926-860X(16)30060-6
DOI: <http://dx.doi.org/doi:10.1016/j.apcata.2016.02.005>
Reference: APCATA 15764

To appear in: *Applied Catalysis A: General*

Received date: 10-9-2015
Revised date: 2-2-2016
Accepted date: 5-2-2016

Please cite this article as: x39c;aria x391;ntonopoulou, Ioannis Konstantinou, Photocatalytic degradation and mineralization of Tramadol pharmaceutical in aqueous TiO₂ suspensions: Evaluation of kinetics, mechanisms and ecotoxicity, Applied Catalysis A, General <http://dx.doi.org/10.1016/j.apcata.2016.02.005>

This is a PDF file of an unedited manuscript that has been accepted for publication. As a service to our customers we are providing this early version of the manuscript. The manuscript will undergo copyediting, typesetting, and review of the resulting proof before it is published in its final form. Please note that during the production process errors may be discovered which could affect the content, and all legal disclaimers that apply to the journal pertain.

**Photocatalytic degradation and mineralization of Tramadol
pharmaceutical in aqueous TiO₂ suspensions: Evaluation of kinetics,
mechanisms and ecotoxicity**

Maria Antonopoulou^{1,2}, Ioannis Konstantinou^{1,2*}

*¹Department of Environmental and Natural Resources Management,
University of Patras, 30100, Agrinio, Greece.*

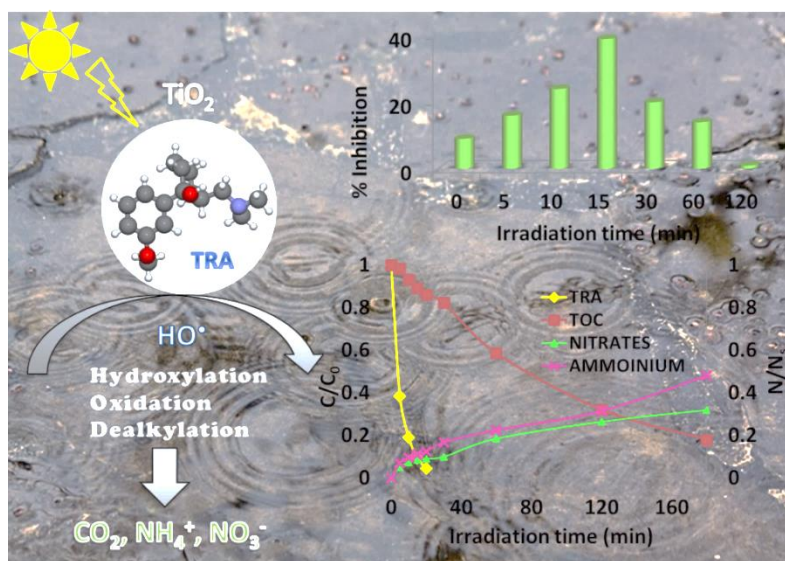
²Department of Chemistry, University of Ioannina, 45110 Ioannina, Greece

*** Corresponding author:**

e-mail: iokonst@cc.uoi.gr; iokonst@upatras.gr

Tel: +30-2651008349

Graphical Abstract



Highlights

- The photocatalytic degradation and mineralization of tramadol was studied.
- Hydroxylation, oxidation and dealkylation were found to be the main transformation pathways.
- HO[•] are the main reactive species during the photocatalytic process.
- Near additive toxicity effects were observed between N-desmethyl, N-oxide tramadol.

ABSTRACT

In the present study the transformation and mineralization of a common aquatic pollutant, Tramadol (TRA) was investigated for the first time by means of TiO₂ photocatalysis. The degradation kinetics for both TRA and total organic carbon (TOC) followed apparent first-order model with rate constants of $k_{app}=15.3 \times 10^{-2} \text{ min}^{-1}$ and $k_{app}=9.7 \times 10^{-3} \text{ min}^{-1}$ and half lives ($t_{1/2}$) of 4.5 min and 71.4 min, respectively. The transformation products (TPs) of TRA, were identified by high resolution accurate mass liquid chromatography (HR-LC-MS) suggesting that hydroxylation, oxidation and dealkylation are the main transformation pathways. The reactions were found to occur mainly at the surface of the photocatalyst via surface-bound HO[•] radicals rather than by free diffusion into the homogeneous phase. The potential risk of TRA and its TPs to aqueous organisms was investigated using Microtox bioassay before and during the process. The acute toxicity increased in the first stages and then decreased rapidly to very low values within 120 min of the photocatalytic treatment. The increase in the toxicity is associated with near additive or low synergistic effects between two TPs generated during the process i.e. N-desmethyl and N-oxide tramadol.

Keywords: Tramadol, photocatalysis, transformation products, ecotoxicity

1. INTRODUCTION

Pharmaceutical compounds are a group of emerging contaminants which are found in surface waters and wastewaters at levels up to a few $\mu\text{g L}^{-1}$, raising major concerns about their potential impact on ecosystems and public health [1-3]. Aquatic toxicity, resistance development in pathogenic bacteria, genotoxicity and endocrine disruption are the main possible adverse effects caused by the frequent occurrence of pharmaceuticals in the aquatic environment [3-6]. Pharmaceuticals are generally designed with high stability for their intended effects on humans and they are poorly removed in wastewater treatment plants (WWTPs) thus, enter the environment as unchanged parent compounds, metabolites or conjugates of both [1, 2]. A representative example of persistent pharmaceutical contaminant is Tramadol (TRA), a centrally acting synthetic opioid analgesic, used worldwide to treat moderate to severe acute or chronic pain. TRA is excreted via urine as an unchanged compound up to 30% and undergoes extensive metabolism, primarily resulting in N-desmethyl- (N-DES) and O-desmethyl- (O-DES) tramadol [6-8].

TRA is partially removed in conventional wastewater treatment plants and as a result it has been frequently detected in sewage outflows as well as in surface water worldwide. According to a European-wide monitoring study on the occurrence of organic micropollutants in WWTP effluents, TRA was one of the most frequent detected contaminants with mean and maximum concentration levels up to 256 and 1116 ng L^{-1} , respectively [5-7].

Advances in water and wastewater treatment have led to the development of promising technologies termed as advanced oxidation processes (AOPs), involving highly reactive hydroxyl radicals (HO^{\bullet}), for the treatment of many emerging contaminants, including pharmaceuticals, poorly eliminated by conventional

biological treatment processes [9, 10]. Heterogeneous photocatalysis using titanium dioxide (TiO_2) as a catalyst is a well-established AOP, providing promising results for both removal and total mineralization of various pharmaceuticals and other micro-pollutants from aqueous phase [11-13]. Heterogeneous photocatalysis typically involves the formation of HO^\bullet , h^+ , HO_2^\bullet , $\text{O}_2^{\bullet-}$, and $^1\text{O}_2$, etc. as oxidizing species and either hydrated electrons (e^-_{aq}) or hydrogen atoms (H^\bullet) as reducing species, which can contribute to the degradation of the contaminants [13-16]. However, only few studies have focused on the identification of photocatalytic transformation products and possible degradation pathways of pharmaceutical compounds [17].

Despite the extensive presence of TRA in various environmental matrices, only a few AOPs such as ozonation and ferrate oxidation [16], electrochemical oxidation [18], and UV/chloramines/ H_2O_2 treatment [19] have been successfully employed for its degradation in aquatic matrices. In the first study, different pathways and major transformation products (TPs) between ozonation and ferrate oxidation were reported while in both cases complete mineralization was not achieved [16]. In the second study, further TPs were formed in the presence of halogen ions while TRA removal was achieved but only a minor reduction of total organic carbon (TOC) was reported [18]. Similarly, different TPs and partial removal of TOC were also observed in the latter study [19].

In this context, no data is currently known regarding the photocatalytic transformation process, the degradation mechanisms and pathways of TRA as well as the toxicity assessment of the treated TRA aquatic solution and its individual transformation products. Photocatalytic reactions proceed via parallel and often interconnected pathways that do not lead always to complete mineralization or detoxification of the treated solution and sometimes more persistent or toxic compounds are formed during

the degradation process [20]; thus the identification and the toxicity assessment of the transformation products are significant milestones for the assessment of the process. Such integrated studies are of great importance for the purposes of proper water and wastewater treatment by photocatalytic process. In addition, oxidation, degradation and transformation of pharmaceuticals via photo-induced reactions (direct and indirect photochemical mechanisms) take place after their release in environmental media. Photocatalytic redox mechanisms are useful for simulating environmental or metabolic degradation processes, thus providing important knowledge on the transformation products of the studied pollutants [21].

The objective of this study was to investigate the photocatalytic degradation of TRA, as a model compound in the opioid analgesics and antidepressants families, providing a fundamental understanding on the applicability and effectiveness of the process for removing the parent compound and transformation products as well as for the detoxification of the aqueous solutions. The transformation kinetics and mechanisms of TRA TiO_2 photocatalytic degradation and mineralization were studied for the first time. The possible degradation pathways of TRA were proposed by identifying the major transformation products using high resolution accurate mass liquid chromatography (HR-LC-MS) and scavenging experiments. The continuous monitoring/assessment of potential toxicity during the treatment was also followed in order to ensure the appropriate degree of treatment and to contribute in the optimization of operating conditions. Moreover, the ecotoxicological potential effects of the major transformation products were determined, providing important knowledge regarding their ecotoxicological potency in aquatic media and giving useful insight on the application of the treatment as additional step in water and wastewater treatment.

In the majority of previously published photocatalytic degradation studies of various pharmaceuticals, toxicity has been generally taken as the overall toxicity of the solution without providing information on potential ecotoxicity of the TPs as well as additives, synergistic or antagonistic effects between them. In this sense, the present work provides various new data regarding the systematic elucidation of the photocatalytic process of this ubiquitous pharmaceutical pollutant in the water.

EXPERIMENTAL SECTION

1.1. Materials

Tramadol hydrochloride salt, anisole and phenol analytical grade (99.9 %) were purchased from Sigma-Aldrich (USA). High purity (99.9 %) standards of N-desmethyl-tramadol (N-DES), N,N-bidesmethyl-tramadol (Bi-DES) and N-oxide-tramadol (N-OX) analytical grade (99.9 %), were purchased from LGC Standards (Germany). Titanium dioxide Degussa P25 (particle size, 20–30 nm; crystal structure, 80% anatase and 20% rutile; surface area, $56 \text{ m}^2\text{g}^{-1}$) was used as photocatalyst. HPLC-grade solvents (acetonitrile, isopropanol, methanol and water) were supplied by Merck (Darmstadt, Germany). Sodium azide (NaN_3), potassium iodide (KI), sodium fluoride (NaF) and potassium dichromate ($\text{K}_2\text{Cr}_2\text{O}_7$) were obtained from Sigma-Aldrich. Superoxide dismutase (SOD) was purchased from Carl Roth GmbH+ Co. KG. (Karlsruhe). HA 0.45 μm filters were supplied by Millipore (Bedford, USA). Oasis HLB (divinylbenzene/N-vinylpyrrolidone copolymer) cartridges (60 mg, 3 mL) from Waters (Mildford, MA, USA) were used for the by-products evaluation.

1.2. Irradiation procedures

Irradiation experiments were performed using a Suntest XLS+ solar simulator (Atlas, Germany). The illumination was performed using a vapor xenon lamp (2.2 kW) equipped with special glass filters restricting the transmission of wavelengths below 310 nm. Photocatalytic degradation of TRA was conducted in a Pyrex reactor with a total volume of 250 mL and a double-walled cooling-water jacket to keep the temperature of the solutions at about 25 °C throughout all experiments. Before illumination, suspensions of TRA solutions (10 mg L⁻¹) containing 100 mg L⁻¹ TiO₂ were stirred at 600 rpm in the dark for 30 min to achieve adsorption–desorption equilibrium.

1.3. Analytical methods

A Dionex P680 HPLC equipped with a Dionex PDA-100 Photodiode Array Detector was used for TRA determination and quantitation. TRA analysis was performed on a Discovery C18, (250 mm length × 4.6 mm ID, 5 µm particle size) column from Supelco (Bellefonte, PA, USA), thermostated at 40 °C. The elution was performed isocratically using LC-grade water at pH 3 (30 %) and acetonitrile (70%) solution as the mobile phase at a flow rate of 1 mL min⁻¹. Quantification was realized at 215 nm. The detection limit was 40 µg L⁻¹ using a signal-to-noise ratio (S/N) equal to 3. TOC removal was followed via a Shimadzu, TOC V-csh Analyzer. NO₃⁻ ions released during the process were determined by a Dionex ICS-1500 equipped with ASRS Ultra II self-regenerating suppressor. Ammonium ions (NH₄⁺) were analyzed by a UV-Vis spectrophotometer (Hitachi, model U-2000) using the colometric method based on indophenol blue formation [22].

1.4. LC-MS analysis

For the identification of TPs, aliquots of 20 mL the irradiated solutions were extracted by means of solid-phase extraction (SPE), using Oasis HLB (divinylbenzene/N-vinylpyrrolidone copolymer) cartridges (60 mg, 3 mL) from Waters (Mildford, MA, USA). SPE was performed using a 12-fold vacuum extraction box (Visiprep, Supelco, Bellefonte, PA, USA). The cartridges were activated and conditioned with 3 mL of methanol and 3 mL LC-grade water at a flow rate of 1 mL min⁻¹. Then, irradiated samples were added at a flow rate of 10 mL min⁻¹ and subsequently dried both by nitrogen stream and vacuum for 15 min. Elution was performed by 2 × 2 mL of methanol. Finally, evaporation of the extracts with nitrogen gas flow to a final volume of 0.5 mL was performed.

The TPs generated during TRA photocatalysis were characterized by an UPLC–ESI-MS system in positive ionization mode. The LC system was equipped with an Accela Autosampler, an Accela LC pump and a LIT Orbitrap mass spectrometer (Thermo Fisher Scientific, Germany). The chromatographic separations were run on a C18 Hypersil Gold, 100 mm x 2.1 mm i.d., 1.9 µm particle size (Thermo Fisher Scientific, San Jose, USA), thermostated at 30 °C. Injection volume was 10 µL and flow rate 300 µL min⁻¹. Gradient mobile phase composition was adopted using water/5mM formic acid as solvent A and methanol/5mM formic acid as solvent B with the following program: 90/10 (kept constant 3 min) to 75/25 in 3.5 min, to 50/50 in 9 min, to 0/100 in 12 min and in 13 min returns to the initial conditions (90/10) and and re-equilibration time was set at 7 min. All ESI-MS experiments were acquired in the positive mode and the ESI-source parameters adopted are stated in our previous work [15]. N-DES- and N-OX-TRA were identified by comparison of retention time, high resolution mass and MS² spectra to the commercially available standards.

2.5. Scavenging experiments for reactive species

0.1 M isopropanol (i-PrOH) was used to scavenge HO[•], 0.1 M methanol was used for quenching h⁺ and HO[•], 0.1 M KI was used to scavenge both h⁺ and surface HO[•]_{ads}, 0.1 mM NaF was used to wash HO[•]_{ads} into solution as bulk HO[•]_{bulk}, 50 μM K₂Cr₂O₇ was used to trap e⁻_{aq} in solution and SOD (100 units mL⁻¹) was used to scavenge O₂^{•-}. Photocatalytic experiments using MeCN solutions were also performed for discrimination between the oxidation by HO[•] and h⁺. Finally, aqueous solutions degassed with high-purity O₂ and N₂ (for e⁻_{aq}) was also photocatalytically treated [23-27].

2.6. Toxicity measurements

For the assessment of the potential impact of TRA and its TPs to aqueous organisms, *Vibrio Fischeri* bioassay was performed before and during the process using a Microtox Model 500 Analyzer (Azur Environmental). A detailed description of the procedure has been reported in our previous study [27]. The toxicity of individual TP's as well as of their mixtures with concentrations levels as those determined during the photocatalytic degradation was also measured in order to discriminate which TP's are more toxic and potential additive or synergistic effects.

3. RESULTS AND DISCUSSION

3.1. Photocatalytic Degradation Kinetics of TRA

Preliminary hydrolysis, adsorption and simulated solar photolysis experiments were carried out in order to determine the contribution of these effects in the overall photocatalytic process. Adsorption experiments carried out in dark with TRA at 10

mg L⁻¹ and TiO₂ at 100 mg L⁻¹, showed no significant adsorption of TRA on the catalyst's surface, i.e. less than 9 %, at equilibrium (30 min). Similarly, hydrolysis experiments showed no significant degradation of the compound. Photolysis experiments under simulated solar light (SSL) without catalyst, using the same initial concentration as in photocatalytic experiments, confirmed that the direct photodegradation is a relatively slow process, and about 29 % of TRA was degraded after 20 min while the corresponding mineralization degree was only 3.75 %. During simulated solar photolysis, TRA molecules can absorb photons as TRA peak maximum absorption at 271 nm tails well over 500 nm overlapping with solar spectrum in the 310–500 nm region.

In contrast, within the same time framework (20 min) the investigated pharmaceutical was degraded very quickly (more than 95% of degradation) in aqueous titanium dioxide suspensions, irradiated with simulated solar light (Fig. 1). Consequently, the observed fast decomposition in the presence of TiO₂ is ascribed to the catalyst's activity. Complete degradation of TRA was achieved within 30 min with a half time of 4.5 min, following an apparent first-order degradation model. In contrast, TOC removal followed a slow rate, showing a half time of 71.4 min. and percentages of approximately 80 % have been achieved only after 240 min irradiation. At this irradiation period, nitrogen was mainly mineralized into NH₄⁺ ions (almost 48 %) and in a lesser extent into NO₃⁻ (almost 30 %). The higher amount of NH₄⁺ ions compared to NO₃⁻ can be explained by the chemical structure of TRA bearing alkyl amine group. According to literature data, the photocatalytic degradation of molecules having alkyl amines as functional groups lead to the generation of a large amount of NH₄⁺ and a minor amount of NO₃⁻ [28, 29]. TiO₂ photocatalytic treatment was demonstrated to be

a suitable tool to remove TRA from the water leading to almost complete mineralization.

3.2. Contribution of Different Reactive Species by scavenging experiments

Several oxidative and reductive species including h^+ , e^- , HO^\bullet , $O_2^{\bullet-}$, 1O_2 , H_2O_2 , 1O_2 , etc. are generated in UV-Vis/TiO₂ photocatalysis that can react with the organic contaminants [14, 15, 23]. The degradation kinetics of TRA in the presence of various scavengers are depicted in Fig. 2, and the variation of pseudo-first-order kinetic parameters in the presence of the employed scavengers is also summarized in Table S1.

Isopropanol, a well-established HO^\bullet scavenger, has been widely used to discriminate the direct oxidation of substrates by hydroxyl radicals due to its high-rate constant reaction with the radical ($1.9 \times 10^9 \text{ M}^{-1}\text{s}^{-1}$) [15, 25]. The rate constant decreased by 95.4% when i-PrOH was added indicating significant contribution of HO^\bullet to TRA degradation.

Methanol can act as HO^\bullet radical scavenger with a rate constant of $1 \times 10^9 \text{ M}^{-1}\text{s}^{-1}$ [30] as well as can be adsorbed on TiO₂ surface and act as an electron donor reacting with photogenerated holes [31]. With MeOH addition, the rate constant decreased notably to $0.4 \times 10^{-2} \text{ min}^{-1}$, showing a reduction of 97.4 % in the rate constant originated from both HO^\bullet and h^+ scavenging. The use of MeCN as reaction media could also help to discern the participation of holes and HO^\bullet in the reaction mechanism. A similar inhibition ($\approx 95 \%$) was observed when TRA photocatalytic degradation was performed in MeCN solution, verifying the participation of HO^\bullet radicals and the limited contribution (about 2.4 %) of direct positive hole oxidation.

I⁻ anions were used to scavenge both h⁺ and surface HO[•]_{ads}, as react steadily with holes and HO[•] leading to iodine formation [25,31]. When I⁻ anions were added to the TRA solution, an inhibition of 92.1 % was observed, suggesting that TRA degradation was mostly induced by HO[•]_{ads}. According to the above mentioned results, the degradation of TRA was found to take place at the surface or at least in the intimate proximity of the TiO₂ particles whereas the participation of HO[•] in bulk water can be assumed minor. The participation of h⁺ on the degradation mechanism is also consistent with the oxidation of TiO₂ surface OH-groups to produce HO[•] radicals. With azide addition, a well-known ¹O₂ and HO[•] scavenger [15], the rate constant decreased by 83.1 % (data not shown). This result indicates that ¹O₂ did not participate apparently in TRA oxidation. In the presence of NaF the observed rate constant was $9.2 \times 10^{-2} \text{ min}^{-1}$, corresponding to 39.9 % inhibition due to the transformation of HO[•]_{ads} to HO[•] bulk [23]. This reduction in the degradation inhibition proves once more that TRA degradation takes place at the surface of the catalyst.

Quenching e⁻_{aq} in the TiO₂ conduction band under SSL irradiation by adding K₂Cr₂O₇, the rate constant decreased to $4.5 \times 10^{-2} \text{ min}^{-1}$ (70.6 % inhibition). In order to clarify the direct or indirect contribution of e⁻_{aq} as well as to exclude the interference of light absorption by K₂Cr₂O₇ further experiments were conducted. A solution containing TRA, I⁻ ions and i-PrOH degassed with N₂ was irradiated excluding all other species except reductive e⁻_{aq} and a rate constant equal to $0.3 \times 10^{-2} \text{ min}^{-1}$ was obtained, indicating that direct e⁻_{aq} reaction could contribute only 2 % in the degradation. To confirm this assumption, TRA degradation was also conducted in presence of I⁻ ions, i-PrOH, and O₂ to transform e⁻_{aq} into the relative oxidative species, the superoxide radical anion (O₂^{-•}). A rate constant of $5.2 \times 10^{-2} \text{ min}^{-1}$ was

observed, indicating a considerable contribution (66 %) of $O_2^{\cdot-}$ to TRA degradation. Similarly, the addition of SOD to the solution, which has been used to quench $O_2^{\cdot-}$ by a simple electron transfer mechanism provokes 67.3 % inhibition of the photocatalytic degradation of TRA, proving once more the indirect contribution of e^-_{aq} . In aqueous solutions the reaction of $O_2^{\cdot-}$ with protons is favorable giving rise to the formation of H_2O_2 which can produced further HO^{\cdot} radicals. Overall, oxidative species, in particular HO^{\cdot} and to a lesser extent $O_2^{\cdot-}$ were predominantly responsible for TRA degradation in aqueous solutions.

Based on the detailed scavenging study, the photocatalytic degradation of TRA proceeds as follows: In the first steps TRA diffuses from bulk solution to the catalyst surface. After the photo excitation of TiO_2 with light energy greater than its band gap energy, conduction band electrons (e^-) and valence band holes (h^+) are generated. The photogenerated holes oxidize adsorbed TRA in a minor extent, but mainly react with OH surface groups oxidizing them into HO^{\cdot} radicals. Subsequent HO^{\cdot} attack on TRA molecule leads to various transformation products before mineralization. On the other hand, the photogenerated electrons react with O_2 adsorbed on the TiO_2 -surface, reducing it to $O_2^{\cdot-}$. Finally, $O_2^{\cdot-}$ could attack TRA or produce more OH^{\cdot} contributing to its degradation.

3.3. Photocatalytic Degradation Mechanism of TRA

The identification of 14 intermediates during TRA degradation by heterogeneous photocatalysis was allowed using UPLC/MS/MS (Table 2S). Structural assignment was based on accurate mass analysis of both pseudo-molecular ion peaks and MS/MS fragmentation patterns with a high grade of accuracy (< 6 ppm error). In UPLC/MS TIC chromatograms (Fig. S1), most of the identified TPs eluted before TRA,

indicating the formation of more hydrophilic TPs. Five species with $[M+H]^+$ ions of m/z 280.1891-280.1904 (280-A,B,C,D,E,) and molecular formula $C_{16}H_{26}NO_3$ were formed, corresponding to the addition of 15.995 mass units to TRA (m/z 264.1949), consistent with TRA mono-hydroxylated products (OH-TRA). In some cases the position of the hydroxylation can be proposed from the analysis of the MS^2 spectra, summarized in Table 2S. All isomeric TPs showed: (a) the formation of a major MS^2 product ion at m/z 262.1804 ($C_{16}H_{24}NO_2$) originating from H_2O loss, as observed also on the fragmentation of TRA molecule; and (b) the presence of a fragment at m/z 217.1224 with a molecular formula of $C_{14}H_{17}O_2$ (loss of C_2H_7N). The latter loss indicates unmodified N,N-dimethylamino group and suggests the hydroxylation of either the cyclohexane or benzene ring and the methylene group attached to the cyclohexane ring. Taking into account that TRA presents a pK_a of 9.41, the tertiary amine group was protonated at the experimental pH (6.7) and the reactivity of this group towards electrophilic species such as HO^\bullet and h^+ can be considered low in consistency with the observed intact tertiary amine group based on the MS data. As regards isomer 280-A, the structural-diagnostic MS ion at m/z 250.1786 ($C_{15}H_{24}NO_2$) fits well with the loss of $CH_2=O$ fragment that is common for aromatic methyl ethers and exclude the methoxy group as an hydroxylation site. Isomers 280B-E presented a MS^2 product ion at m/z 149.0230-149.0241 with a chemical formula of $C_8H_5O_3$ which is indicative for hydroxylation of the aromatic ring. Mono-hydroxy derivatives have also been identified during ozonation [16] as well as electrochemical oxidation [18] of TRA. Based on NMR analysis of the dehydrated OH-TRA, Eversloh et al. [18] suggested that hydroxylation of TRA during electrochemical oxidation occurred in the benzene ring in para and ortho orientation to the methoxy group. On the contrary, Radjenovic et al. [19] did not observed hydroxylation of the methoxybenzene moiety

during UV/H₂O₂/chloramine treatment and the elucidated by-products indicated mostly oxidative transformations at the cyclohexane ring relied on the observed successive losses of water.

Simultaneously, the three peaks eluted at 4.98, 5.89 and 6.38 min with a molecular formula of C₁₆H₂₆NO₄ and a pseudo-molecular ion of 296.1844 (296A,B,C) were also detected on the basis of the insertion of two hydroxyl groups (31.9990 units mass difference comparing to original TRA molecule) and attributed to di-hydroxylated TRA. For TPs 296A,B, successive losses of water in MS² fragmentation were observed. Consequently, it is suggested that one OH-group is located in the cyclohexane moiety as reported also for other dihydroxylated TRA TPs in Radjenovic et al. [19]. Further hydroxylation of TRA leads to the formation of one TP with [M+H]⁺ ion of m/z 312.1818 (C₁₆H₂₆NO₄) at the first stages of the photocatalytic treatment. In this case the very small concentration hampered further structural elucidation. Multiple hydroxylation of TRA has also been reported during electrochemical oxidation [18]. Oxidized TPs was formed simultaneously or consecutively with the formation of mono-hydroxylated derivate with [M+H]⁺ 278.1887 and empirical formula of C₁₆H₂₄NO₃. A TP with [M+H]⁺ 278.1751 was also detected during ozone and Fe(VI) treatment of TRA [16] and it is assigned to the transformation of the methyl group in the amine moiety to an aldehyde group.

The three TPs eluted at 7.90, 7.92 and 5.76 min were identified as N-DES, N-OX- and O-DES-TRA, three well-known metabolites of TRA. The formation of N-DES and N-OX during treatment was also confirmed by comparing R_t, nominal masses as well as MS² spectra with the authentic reference standards. The above mentioned TPs had been also previously identified as major transformation products of ozonation [16] and electro-oxidation of TRA [18]. In addition, they have been detected as

transformation products of TRA after entering the aquatic environment in its unchanged structure as a result of biotic and abiotic processes [6-8].

The formation of N-OX can be explained by the well-documented in the literature oxygen transfer mechanism. The oxidation of tertiary amines by oxygen transfer to the corresponding N-oxide has also been reported for different oxidants such as Fe(VI), [16] O₃ [16, 32, 33] and MnO₄ [33-34]. The dealkylation mechanism (N-DES, O-DES) involves the initial hydroxyl radical attack on the methyl group and the subsequent formation of hydroperoxide and aldehyde structures. Further oxidation of the aldehyde TPs followed by decarboxylation reactions justify the generation of N- and O- dealkylated TRA [35-37].

Using HPLC–DAD system, later stage TPs, anisole and phenol, were determined. The formation of both anisole and phenol was validated by the retention times and the UV-vis spectra of the commercial standards under the same chromatographic conditions. Anisole is generated via the oxidative opening and subsequent dealkylation reactions of cyclohexane moiety of TRA. Various TPs with oxidative cyclohexane ring opening have been identified in Radjenovic et al. [19] for UV/H₂O₂/chloramine treatment. Thereafter, phenol is generated from anisole by a dealkylation reaction or by cleavage of methoxy group and the subsequent electrophilic addition of the HO[•] radical.

TPs evolution as a function of irradiation time was also followed and the evolution profiles are depicted in Fig. 3. Most of these TPs were readily transformed and after 30 min of irradiation they were completely abated. On the basis of calibration curves created for the TPs with available standards, the maximum concentration of N-OX- and N-DES-TRA was determined to be 2 and 52 µg L⁻¹.

Our data shows that mono- and poly- hydroxy TRA displayed maximum concentrations within the same time scale (15 min) implying that mono- and poly-hydroxylation took place simultaneously. Oxidised (keto or aldehydes) and dealkylated derivatives attained their maximum response within the same time-scale periods, indicating the fast kinetics in the successive reaction network followed during the photocatalytic reaction. Anisole and phenol were formed slowly after successive hydroxylation and oxidative cleavage of cyclohexane ring. Thus, these oxidation products presented their maximum concentration (14 and 18 $\mu\text{g L}^{-1}$ for phenol and anisole, respectively) at prolonged irradiation period of 60 min.

Based on the structures of the TPs discussed above, three different pathways were proposed as depicted in Scheme 1 and include: (a) oxidation of tertiary amine functional group by oxygen transfer mechanism; (b) hydroxylation that occurred mainly in the aromatic and/or cyclohexane ring and (c) oxidation of the alkyl-groups to the corresponding aldehyde structures and subsequent demethylation of the N- and O-alkyl chain.

After prolonged irradiation time, these TPs are further decomposed into other low-molecular-weight products such as anisole and phenol. The last step involves oxidative opening of the aromatic ring, leading to lower molecular weight aliphatic products such as carboxylic acids [38]. Although, the final aliphatic transformation products were not possible to be identified by the employed analytical instrumentations, the evolution of nitrogen ions and TOC removal confirm the cleavage of the rings and the formation of nitrogen containing and de-nitrogenated aliphatic by-products. Carboxylic acids such as maleic, oxalic, formic, fumaric have been reported as final products of phenol and phenolic-type derivatives degradation.

Total mineralization of these aliphatic carboxylic acids proceeds through the loss of a CO₂ molecule via the well-established photo-Kolbe reaction in the literature [38].

3.4. Ecotoxicity evolution

The toxicity evolution during photocatalytic degradation is essential for assessing the feasibility of water treatment techniques [19]. Aquatic toxicity is an important parameter in assessing the potential adverse effects of chemicals and complex mixtures on aquatic species and ecosystems, thus the acute toxicity of TRA and its transformation products was monitored with the *Vibrio Fischeri* toxicity test. The toxicity of initial TRA solution and of the treated samples was measured after 5, 15 and 30 min of exposure to the tested organism. Since no difference in the measurements between different exposure periods was observed, in Fig. 4A the inhibition measured after 15 min of contact time is depicted. No variability in toxicity measurements between the different exposure times has also been observed in previous studies which used *Vibrio Fischeri* bioassay as toxicity test [27, 39, 40]. Although the original solution is relatively non-toxic to *Vibrio Fischeri* (9 % inhibition), toxicity increased during the first stages reaching the inhibition value of about 40 % up to 15 min of the photocatalytic reaction to progressively decrease thereafter. The toxicity profile did not follow the trend of the degradation of TRA indicating the formation of toxic transformation compounds that were eliminated at longer prolonged irradiation times. Notably, the observed % inhibition was found to attain its maximum value in 15 min, simultaneously with the highest abundance of the majority of the identified TPs.

In an attempt to identify the intermediates responsible for increased toxicity, the toxic effect of two of the most abundant and commercial available TPs identified, N-DES-,

and N-OX-TRA towards *Vibrio Fischeri* was investigated. The concentrations investigated were equal to their maximum concentrations determined after 15 min. According to the results depicted in Fig. 4B, these TPs, showed lower toxicity compared to TRA, presenting 6 % and 4 % inhibition, respectively.

In order to investigate possible additive or synergistic effects, mixture solutions containing TRA and the two TPs at concentrations equal to those detected during the photocatalytic experiments after 15 min were prepared. The solution showed an inhibition of 26 % indicating near additive or low synergistic effects between them. After 30 min of photocatalytic treatment toxicity is decreased and at 120 min detoxification is achieved reaching the value of 3% inhibition. Acute toxicity test using *Vibrio Fischeri* bioassay highlights the efficiency of the photocatalytic process in the detoxification of the irradiated solution. The results clearly demonstrate that the potential risk of TPs and the toxicity evolution demands special consideration during the evaluation and planning of water treatment technologies.

4. CONCLUSIONS

Heterogeneous photocatalysis was demonstrated to be an efficient treatment technology for removing TRA, a representative pharmaceutical pollutant from the water. Simultaneously with the total abatement of TRA, high percentages of mineralization were accomplished. HO[•] radicals were found to be the most important species, attacking TRA molecule non-selectively, during the process. Using advanced mass spectroscopy techniques, a great number of hydroxylated, oxidized and dealkylated TPs were identified. The potential adverse effect of the treated solution during the process was studied using Microtox bioassay. An increase in the toxicity

was observed in 15 min and attributed to near additive or low synergistic effects between N-desmethyl and N-oxide tramadol.

Acknowledgements

This research has been co-financed by the European Union (European Social Fund – ESF) and Greek national funds through the Operational Program "Education and Lifelong Learning" of the National Strategic Reference Framework (NSRF) - Research Funding Program: THALIS. Investing in knowledge society through the European Social Fund.

The authors would like to thank the Unit of Environmental, Organic and Biochemical high resolution analysis-orbitrap-LC-MS analysis of the University of Ioannina for providing access to the facilities.

REFERENCES

- [1] B. Kasprzyk-Hordern, R.M. Dinsdale, A.J. Guwy, *Water Res.* 43 (2009) 363-380.
- [2] A. Jelic, M. Gros, A. Ginebreda, R. Cespedes-Sánchez, F. Ventura, M. Petrovic, D. Barceló, *Water Res.* 45 (2011) 1165-1176.
- [3] M. Gros, M. Petrović, D. Barceló, *Anal. Chem.* 81 (2009) 898–912.
- [4] E. Stackelberg, E.T. Furlong, M.T. Meyer, D. Zaugg, A.K. Henderson, D.B. Reissman, *Sci. Total Environ.* 329 (2004) 99-113.
- [5] R. Loos, R. Carvalho, D.C. António, S. Comero, G. Locoro, S. Tavazzi, B. Paracchini, M. Ghiani, T. Lettieri, L. Blaha, B. Jarosova, S. Voorspoels, K. Servaes, P. Haglund, J. Fick, R.H. Lindberg, D. Schwesig, B.M. Gawlik, *Water Res.* 47 (2013), 6475-6487.

- [6] P.C. Rúa-Gómez, W. Püttmann, *J. Environ. Monit.* 14 (2012) 1391-1399.
- [7] P.C. Rúa-Gómez, W. Püttmann, *Chemosphere* 90 (2013) 1952-1959.
- [8] M. Bergheim, R. Gieré, K. Kümmerer, *Environ. Sci. Pollut. Res.* 19 (2012) 72-85.
- [9] S. Esplugas, D.M. Bila, L.G.T. Krause, M. Dezotti, *J. Hazard. Mater.* 149 (2007) 631-642.
- [10] M. Klavarioti, D. Mantzavinos, D. Kassinos, *Environ. Int.* 35 (2009) 402-417.
- [11] H. Yang, G.Y. Li, T.C. An, Y.P. Gao, J.M. Fu, *Catal. Today* 153 (2010) 200-207.
- [12] F. Mendez-Arriaga, S. Esplugas, J. Gimenez, *Water Res.* 42 (2008) 585-594.
- [13] D.A. Lambropoulou, M.D. Hernando, I.K. Konstantinou, E.M. Thurman, I. Ferrer, T.A. Albanis, A.R. Fernandez-Alba, *J. Chromatogr. A.* 1183 (2008) 38-48.
- [14] I.K. Konstantinou, T.A. Albanis, *Appl. Catal. B: Environ.* 49 (2004) 1-14.
- [15] M. Antonopoulou, A. Giannakas, Y. Deligiannakis, I. Konstantinou, *Chem. Eng. J.* 231 (2013) 314-325.
- [16] S.G. Zimmermann, A. Schmukat, M. Schulz, J. Benner, U.V. Gunten, T.A. Ternes, *Environ. Sci. Technol.* 46 (2012) 876-884.
- [17] D. Kanakaraju, B.D. Glass, M. Oelgemöller, *Environ. Chem. Lett.* 12 (2014) 27-47.
- [18] C.L. Eversloh, M. Schulz, M. Wagner, T.A. Ternes, *Water Res.* 72 (2015) 293-304.
- [19] J. Radjenovic, M.J. Farré, W. Gernjak, *Environ. Sci. Technol.* 46 (2012) 8356-8364.
- [20] G. Li, X. Nie, Y. Gao, T. An, *Appl. Catal. B: Environ.* 180 (2016) 726-732.
- [21] C-S. Kuo, C-F. Lin, P-K.A. Hong., *J. Hazard. Mater.* 301 (2016) 137-144.
- [22] L. Solorzano, *Limnol. Oceanogr.* 14 (1969) 799-801.

- [23] H. Fang, Y. Gao, G. Li, J. An, P.K. Wong, H. Fu, S. Yao, X. Nie, T. An, *Environ. Sci. Technol.* 47 (2013) 2704–2712.
- [24] H.C. Zhang, C.H. Huang, *Environ. Sci. Technol.* 39 (2005) 4474-4483.
- [25] R. Palominos, J. Freer, M.A. Mondaca, H.D. Mansilla, J. *Photochem. Photobiol. A: Chem.* 193 (2008) 139–145.
- [26] J.P. Raja, A. Bozzi, H. Mansilla, J. Kiwi, J. *Photochem. Photobiol. A: Chem.* 169 (2005) 271–278.
- [27] M. Antonopoulou, I. Konstantinou, J. *Photochem. Photobiol. A: Chem.* 294 (2014) 110-120.
- [28] S. Horikoshi, N. Watanabe, M. Mukae, H. Hidaka, N. Serpone, *New. J. Chem.* 25 (2001) 999-1005.
- [29] P. Calza, E. Pelizzetti, C. Minero, J. *Appl. Electrochem.* 35 (2005) 665–673.
- [30] R. Hazime, C. Ferronato, L. Fine, A. Salvador, F. Jaber, J.-M Chovelon, *Appl. Catal. B: Environ.* 126 (2012) 90–99.
- [31] E.M. Rodríguez, G. Márquez, M. Tena, P.M. Álvarez, F.J. Belt, *Appl. Catal. B: Environ.* 178 (2015) 44–53
- [32] B. De Witte, H. Van Langenhove, K. Hemelsoet, K. Demeestere, P. De Wispelaere, V. Van Speybroeck, J. Dewulf, *Chemosphere* 76 (2009) 683-689.
- [33] F. Lange, S. Cornelissen, D. Kubac, M.M. Sein, J. von Sonntag, C.B.Hannich, A. Golloch, H.J. Heipieper, M. Möder, C. von Sonntag, *Chemosphere* 65 (2006) 17-23.
- [34] K.A. Thabaj, S.D. Kulkarni, S.A. Chimatadar, S.T. Nandibewoor, *Polyhedron* 26 (2007) 4877-4885.
- [35] I.K. Konstantinou, T. M. Sakellarides, V. Sakkas, T.A. Albanis, *Environ. Sci. Technol.* 35 (2001) 398-405.

- [36] M.V.P. Sharma, V.D. Kumari, M. Subrahmanyam, *Chemosphere* 72 (2008) 644–651.
- [37] E. Pelizzetti, C. Minero, V. Carlin, M. Vincenti, E. Pramauro, M. Dolci, *Chemosphere* 24 (1992) 891–910.
- [38] A. Ortiz-Gomez, B. Serrano-Rosales, H. de Lasa, *Chem. Eng. Sci.* 63 (2008) 520–557.
- [39] V.P. Utkigar, N. Chaudhary, A. Koeniger, H.H. Tabak, J.R. Haines, R. Govind, *Wat. Res.* 38 (2004) 3651-3658.
- [40] D.D. Deheyn, R. Bencheikh-Latmani, M.I. Latz, *Environ. Toxicol.* 19 (2004) 161-178.

Legend of Figures-Schemes

Figure 1. Kinetics of TRA photocatalytic degradation and mineralization as expressed by TOC removal and evolution of NO_3^- and NH_4^+ ions (Experimental conditions: initial concentration of Tramadol $[\text{C}_0]=10 \text{ mg L}^{-1}$, concentration of catalyst $[\text{TiO}_2]=100 \text{ mg L}^{-1}$, Irradiation intensity, $I=500 \text{ W m}^{-2}$) (N/N_s = determined concentration of N-species (NH_4^+ , NO_3^-) in each sampling interval/theoretical stoichiometric concentration of N-species formed after mineralization of the initial tramadol concentration).

Figure 2. Degradation kinetics of TRA ($\text{C}_0=10 \text{ mg L}^{-1}$) in the presence of different scavengers in aqueous TiO_2 suspensions (100 mg L^{-1}) under simulated solar light ($I=500 \text{ W m}^{-2}$).

Figure 3. Evolution profiles of TPs (structure assignment as shown in Scheme 1) identified by liquid chromatography- accurate mass spectrometry during the photocatalytic degradation of TRA (conditions: $[\text{C}_0]=10 \text{ mg L}^{-1}$, $[\text{TiO}_2]=100 \text{ mg L}^{-1}$, $I=500 \text{ W m}^{-2}$); A), B), C) LC-ESI-MS peak area as a function of irradiation time; D) concentration as a function of irradiation time.

Figure 4. % Inhibition of luminescence of *Vibrio Fischeri* marine bacteria; A) as a function of photocatalytic treatment ($[\text{TRA}]=10 \text{ mg L}^{-1}$, $[\text{TiO}_2]=100 \text{ mg L}^{-1}$, $I=500 \text{ W m}^{-2}$); B) in the presence of TRA and the detected TPs with available reference standards in concentrations equal to those detected in 15 min of photocatalytic treatment.

Scheme 1. Proposed photocatalytic degradation pathways of TRA in aqueous TiO₂-P25 suspensions.

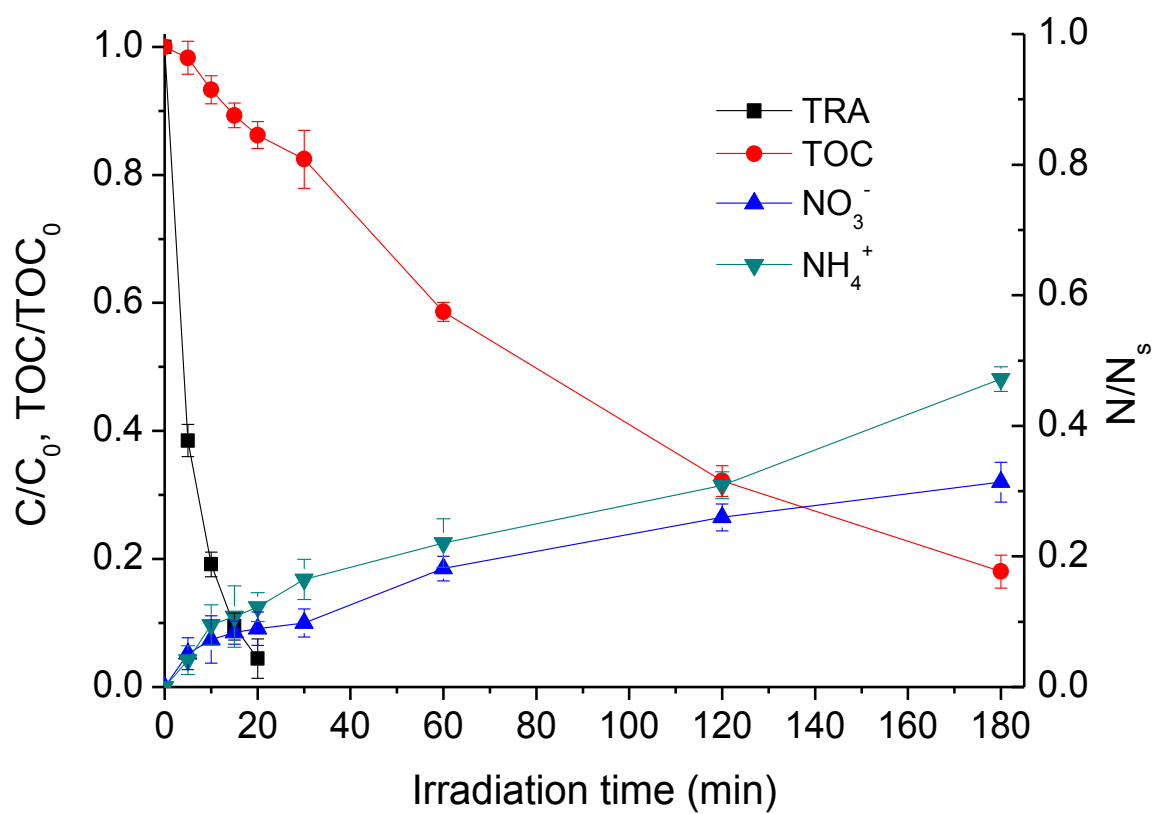


Figure 1.

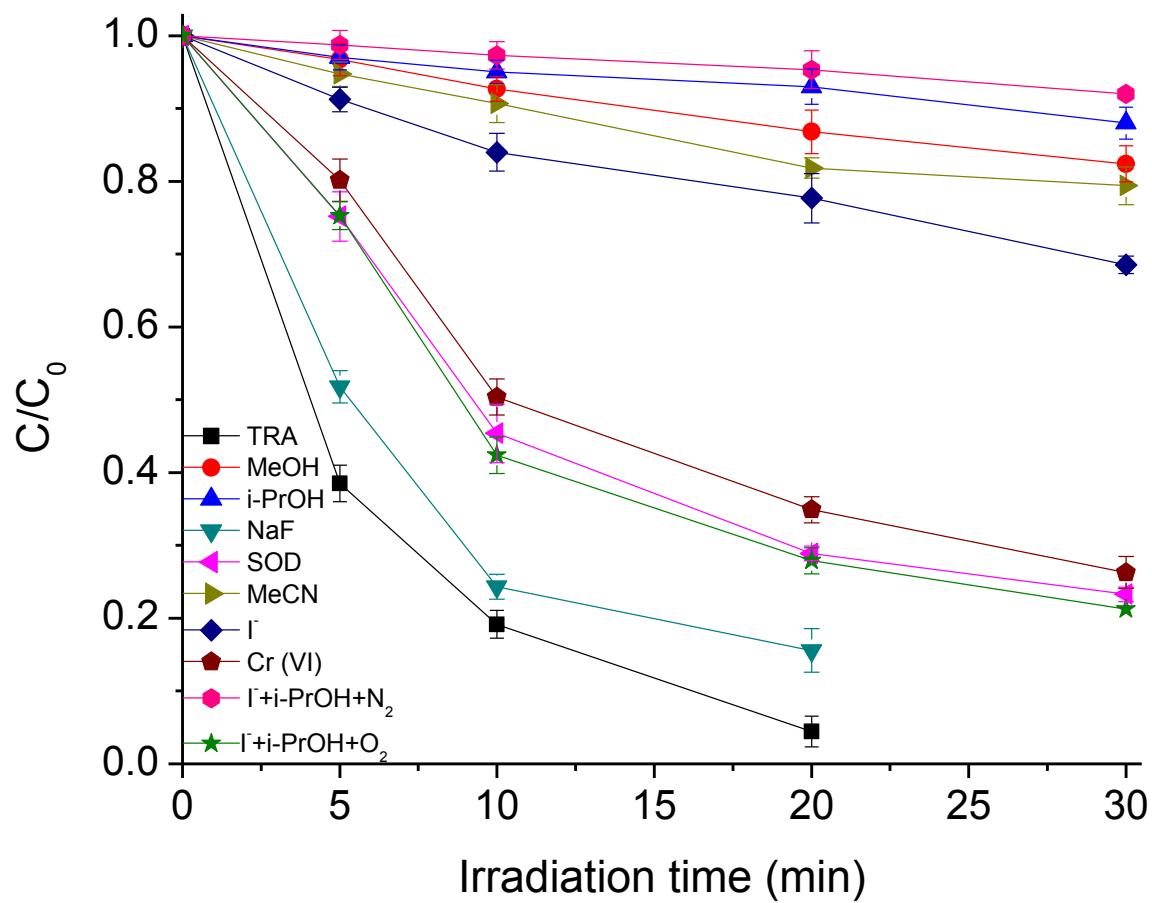


Figure 2.

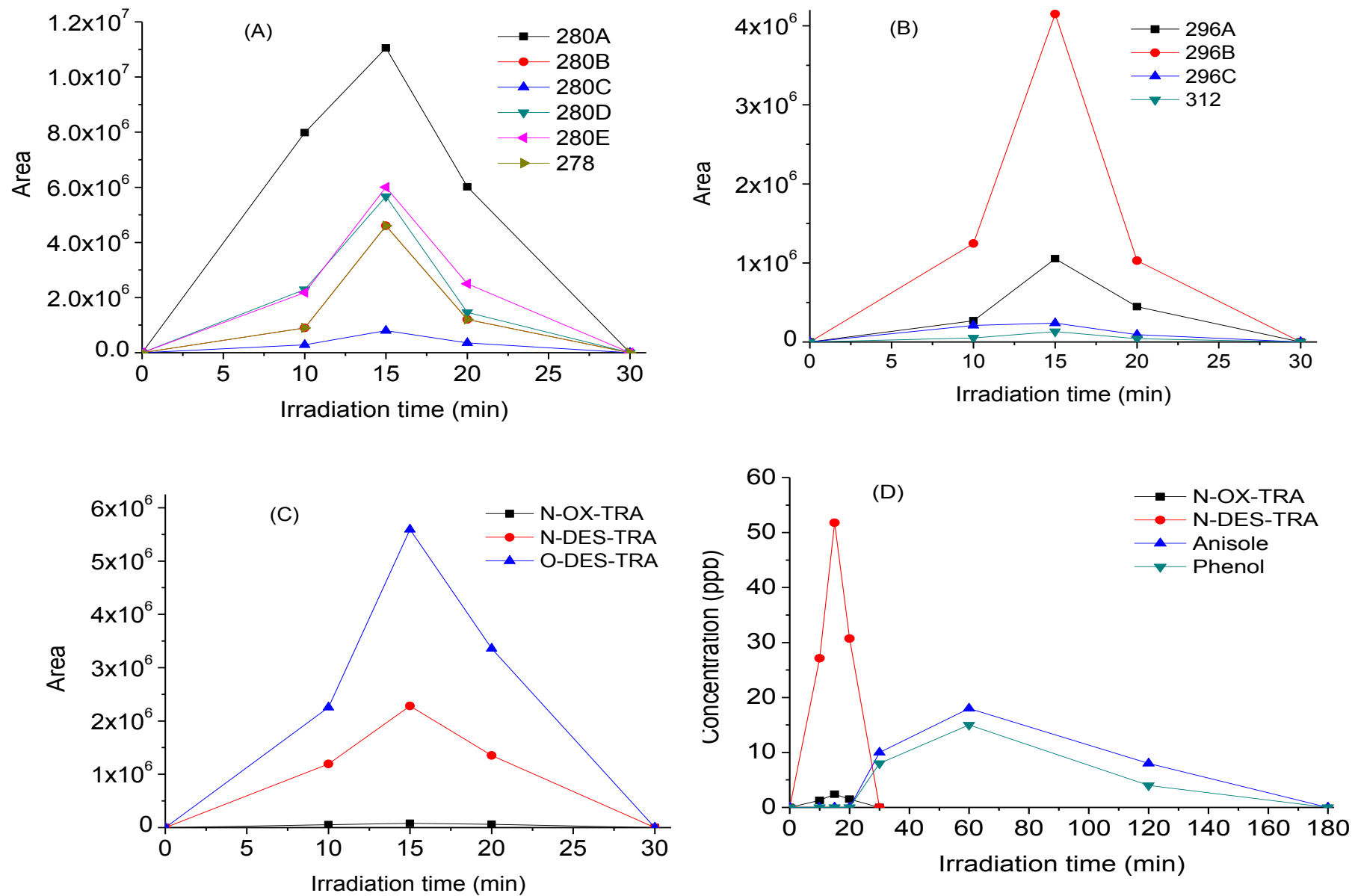


Figure 3.

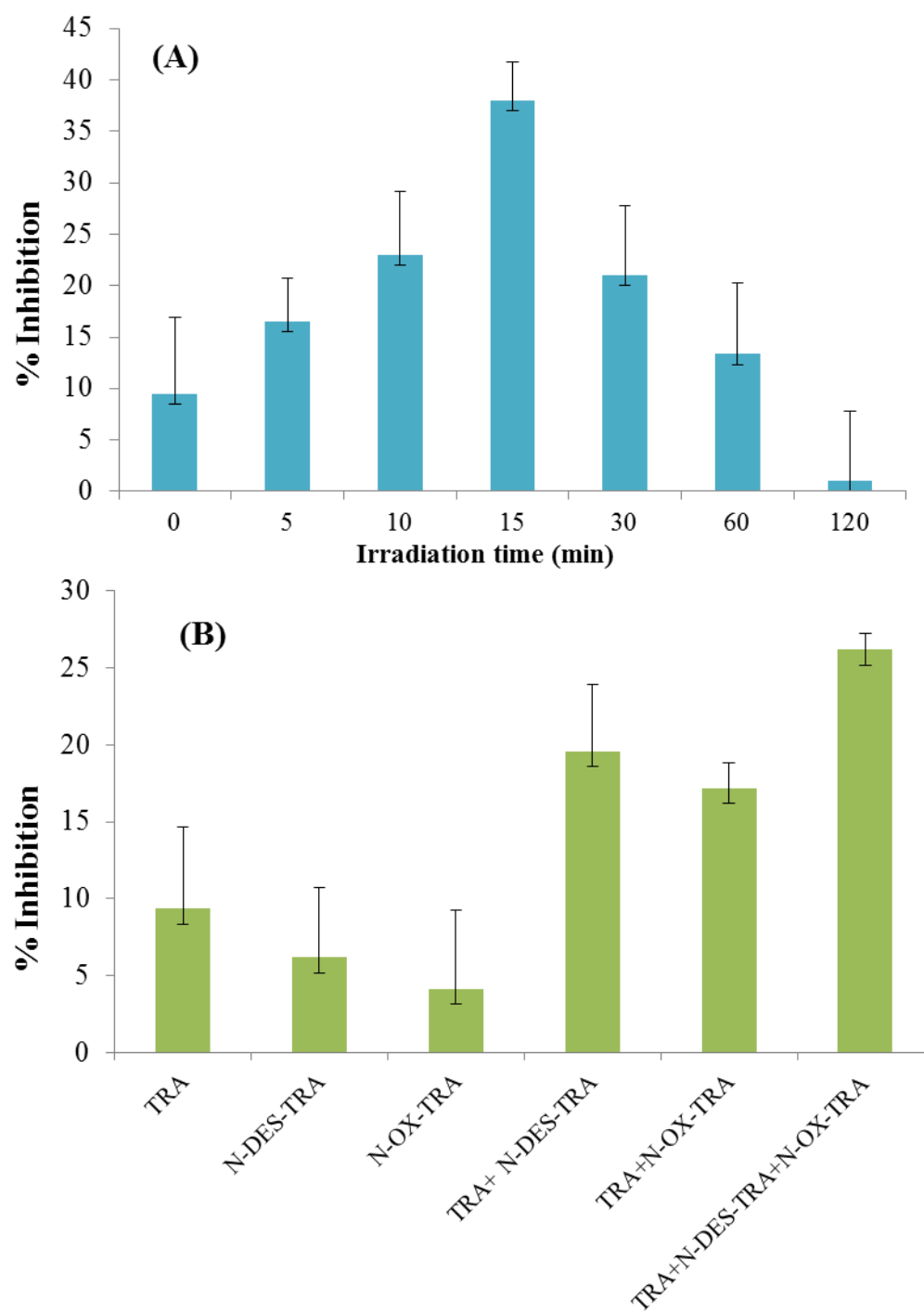
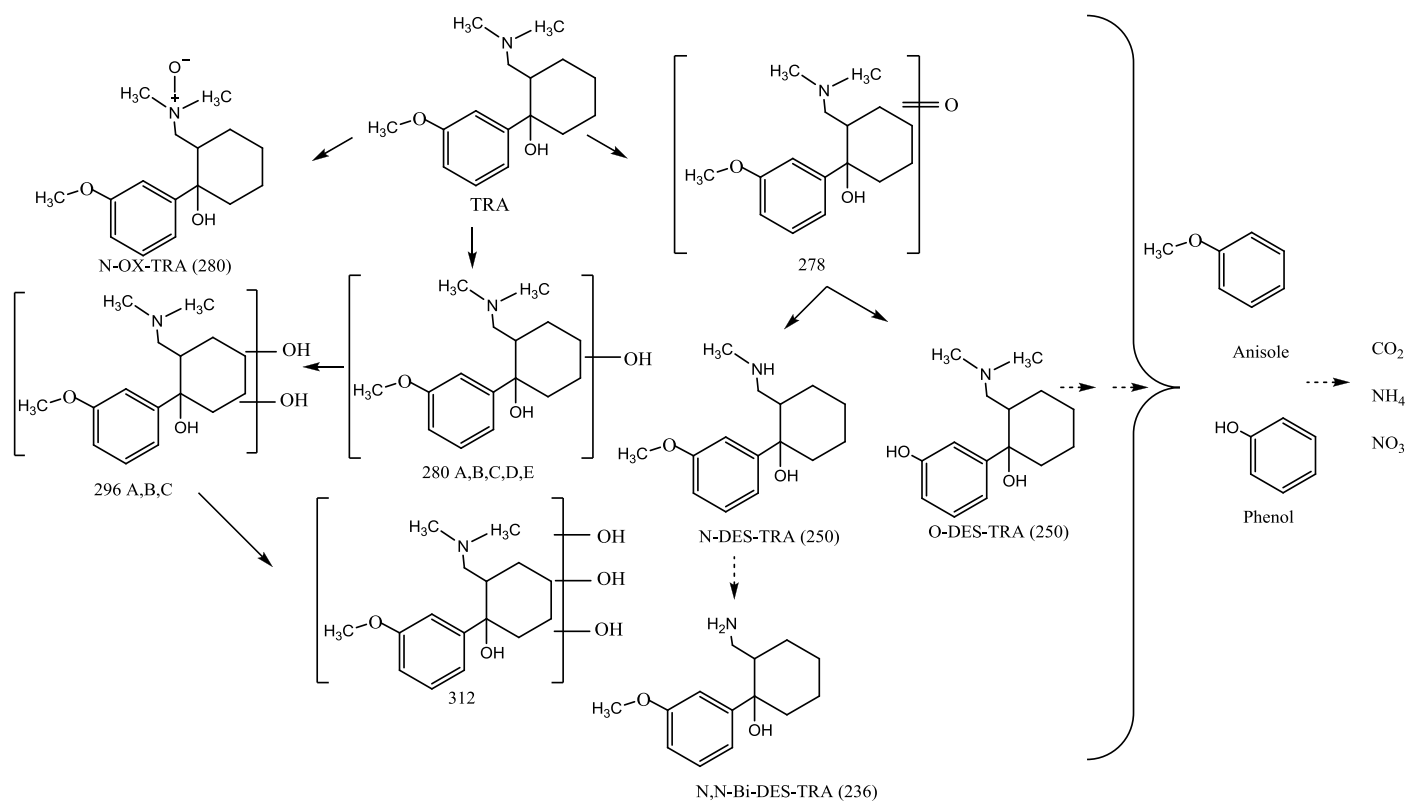


Figure 4.



Scheme 1.